



Bimodal Q-band Probehead with Improved Signal-to-Noise Ratio in Pulse EPR

Vasyl Denysenkov¹, Alexey Fedotov², Burkhard Endeward¹, Thomas F. Prisner¹

¹Institute for Physical and Theoretical Chemistry, Goethe University Frankfurt, 60438, Germany

²A.V. Gaponov-Grekhov Institute of Applied Physics of the Russian Academy of Sciences, Nizhny Novgorod, 603950, Russia

Correspondence to: Vasyl Denysenkov (Denysenkov@em.uni-frankfurt.de)

Abstract. In addition to the development of various resonators, the concept of a probehead equipped with an additional low noise amplifier (LNA) is becoming increasingly popular to enhance the sensitivity of EPR spectrometers. The low noise detection amplifier makes it possible to measure pulsed EPR signals with high sensitivity. However, a strong reflected pulse signal can cause saturation and deterioration of the LNA characteristics, which requires protection of the LNA (for example, by using a protection switch in front of the LNA), which in turn reduces the signal-to-noise ratio. To overcome these limitations, we propose using an EPR probehead based on a bimodal cavity with strong isolation between the input and output ports, in combination with a low noise amplifier connected to the cavity output. Experiments demonstrate 4-fold increase in the signal-to-noise ratio (SNR) compared to the reflection mode. Performance of the probe was also compared with the Bruker EN 5170 D2 probe available in our laboratory, which showed an improvement that can be achieved by increasing the SNR by 2 times due to additional LNA and isolation of the detection channel from the input signal, and by 3.3 times due to a larger sample volume in the bimodal probe (~20 μ l) at Q-band frequencies compared to the Bruker one (~6 μ l).

The developed probehead can be used together with commercial Bruker ELEXYS EPR spectrometers without modification of the microwave bridge.

20 1 Introduction

Electron paramagnetic resonance (EPR) spectroscopy is a well-established method for studying systems with unpaired electrons. It is widely used in research areas such as chemistry, physics, medicine, biology, and materials science. Increasing the sensitivity of EPR spectrometers is important for the development of new methods that open up new application possibilities.

25 The central component of any conventional EPR spectrometer is a resonator, which amplifies the excitation as well as the induced microwave (mw) signal in the sample, thereby determining the sensitivity of measurements. Single-mode cavities (Reijerse et al., 2012) and dielectric resonators (Hyde and Mett, 2017; Raitsimring et al., 2012) are the most commonly used resonators operating in the reflection mode, which are used in almost all EPR spectrometers. For some specific applications, more sophisticated options such as loop-gap resonators (LGR) (Hyde and Froncisz, 1989; Rinard and Eaton, 2005; Simovic et al., 2006; Forrer et al., 2008; Tschaggelar et al., 2017), photonic band gap resonators (Milikisiyants et al., 2018), plasmonic



metasurface resonators (Tesi et al., 2021), microresonators (Usevicius et al., 2025; Twig et al., 2013), Fabry-Perot resonators (Tipikin et al., 2010; Neugebauer and Barra, 2010; Budil and Earle, 2004) were developed for measurements in reflection mode depending on the used mw frequency range and the condition of the sample. A further example is a dual-mode cavity that matches both mw excitation frequencies in experiments with pulsed electron electron double resonance (PELDOR/DEER), 35 which increases the sensitivity of such experiments with a large frequency separation of the mw excitation pulses (Tkach et al., 2011). However, when operating in reflection mode, a significant part of the mw excitation power returns to the mw bridge due to resonator ring-down under pulse EPR conditions, and may reduce the sensitivity of the spectrometer receiver due to insertion losses in the protection gate switches in pulse mode, and due to the mw source noise in continuous wave (CW) mode. 40 A well-known approach to avoid the ringing as well as to reduce the problem with the source noise is the use of a bimodal cavity in which two modes with orthogonal H-field polarization resonate at the same frequency permitting detection of the orthogonal component of the circularly polarized induction signal, i.e. to excite the x-component of the magnetization and to detect the y-component (Huisien and Hyde, 1974; Mailer et al., 1980; Barendswaard et al., 1984; Prisner and Dinse, 1989). This approach has also been used with loop-gap resonators (Piasecki et al., 1996) and cross-loop resonators (Rinard et al., 1996), as well as for a non-resonant probehead (Smith, et al., 2008). 45 Another key element for determining the SNR of the detected EPR signal is a low noise amplifier (LNA) used directly after the resonator. It is becoming increasingly popular to improve spectrometer sensitivity (Bienfait, et al., 2016; Pfenninger et al., 1995; Simenas et al., 2021; Kalendra et al., 2023; Jbara et al., 2025; Rinard et al., 1999). An additional LNA inserted into the probehead can help to minimize noise contribution of the circulator or any similar transmit/receive decoupling circuit, as well 50 as a protection switch for the LNA inside the mw bridge of the EPR spectrometers. In principle, if the LNA is used as the first device after the resonator, then all other components no longer play any significant role for the SNR. However, in most cases, the compatibility of such probes with commercial EPR spectrometers becomes a non-trivial task requiring some modification of the mw bridge. In particular, strong ring-down signal can lead to the LNA saturation or damage, while protection switches, in turn, result in additional noise. Here we demonstrate the use of a bimodal cavity embedded in a Q-band probe, combined 55 with an additional LNA to improve the sensitivity of a Q-band EPR spectrometer. For our test measurements, the LNA is placed outside the cryostat at room temperature to avoid complications caused by the external static magnetic field and low temperatures. The probehead can be used with commercial EPR spectrometers without any modification of the setup. The probe was tested by pulsed EPR with various samples at room temperature and at 80 K. The isolation between the excitation and detection mode makes it possible to take full advantages of the LNA and noticeably improve the sensitivity of the spectrometer.

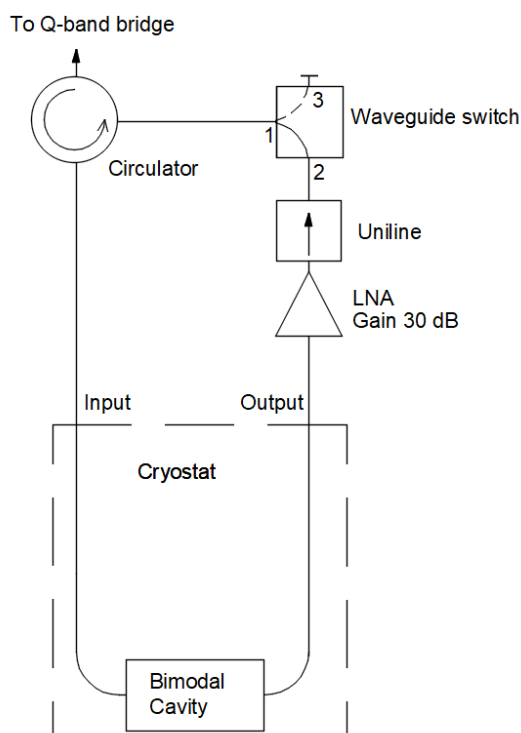
60 2 Development of the probehead

The probehead is designed to be compatible with the Bruker ELEXYS E580 EPR spectrometer and operate inside a CF935 cryostat (Oxford Instruments, UK) at temperatures in the range of 5 – 300 K.



We use a bimodal cavity based on the design described by James Hyde and coworkers, scaling it up for Q-band applications. This is a bimodal cavity in which two rectangular TE103 modes are polarization-crossed and have two half-wavelengths 65 common (Hyde et al., 1968). The great merit of this kind of cavity is the significant isolation between the input and output modes that can be achieved with sample volume of 20-50 microliters over a wide temperature range.

The block-diagram of the probehead with a cavity is shown in the Fig. 1. The probe can be connected to the Q-band bridge of the Bruker ELEXSYS E580 EPR spectrometer by means of a standard WR-28 waveguide.



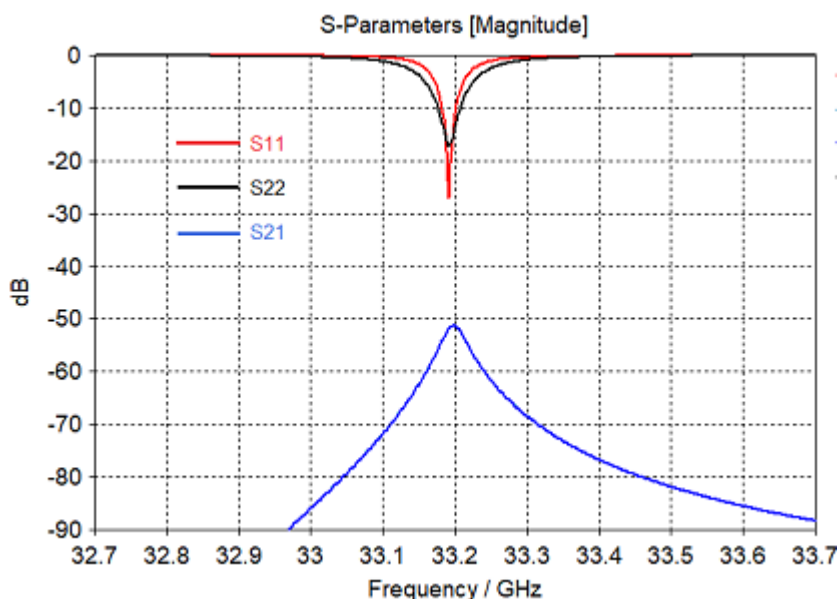
70 **Figure 1: Block-diagram of the Q-band EPR probehead. The waveguide switch is shown in the position 1-2 for transmission mode operation. Reflection mode is available when the switch is in the position 1-3.**

The probehead can operate in reflection or transmission mode, depending on the position of the manual waveguide switch (530B/383 MI-Wave Inc., USA). The reflection mode of operation is typical for conventional probes and will not be described further here. In transmission mode the probehead operates in combination with a LNA. Our used LNA (Model JS-426004000-75 27-10P Narda-MITEQ, USA) has a 1.9 dB noise figure at 20 °C, which corresponds to an equivalent noise temperature of 160 K. For our test experiments it is placed outside the sample cryostat. The uniline (4IWN32-2 Dorado Int., USA) protects the LNA from reflected mw power. A circulator (Model 179B-34/383 Anritsu Inc., Japan) with 0.13 dB insertion loss and 33 dB isolation at 34 GHz was chosen to direct the mw power from the Q-band bridge to the bimodal cavity and from the LNA back to the receiver part of the spectrometer.



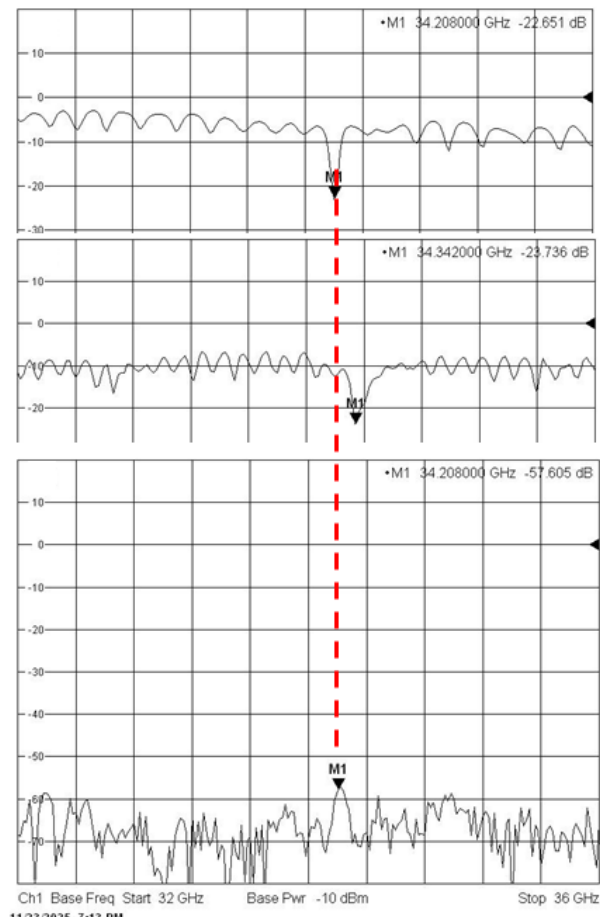
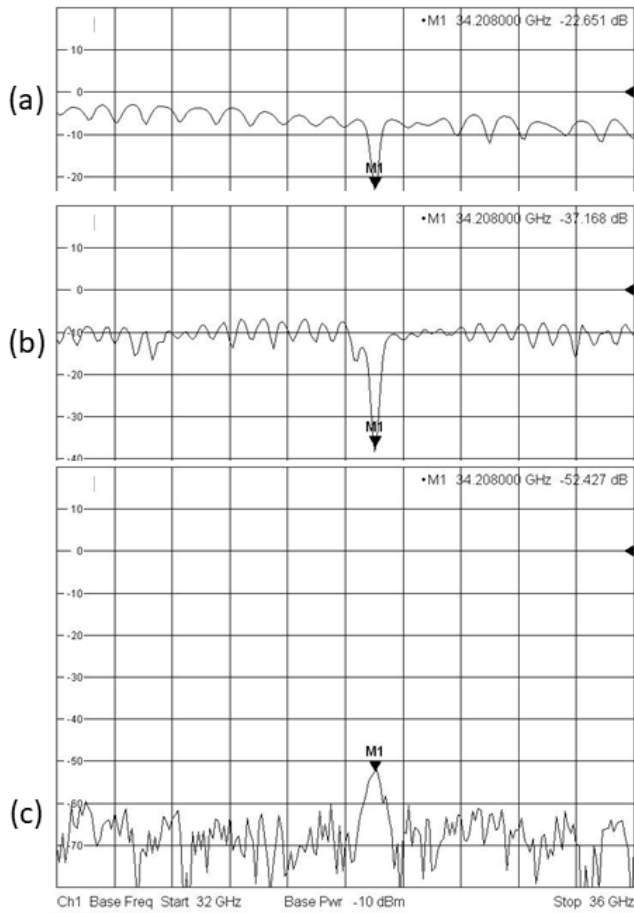
80 3 Experimental results

The probehead loaded with a frozen aqueous solution (with a dielectric constant of $\epsilon = 3.4$ and a loss tangent of $\text{tg}\delta = 0.01$) in a quartz sample tube has been simulated in the 33 - 34.5 GHz range by finite element calculations with CST Suite version 2021. The simulation results are frequency-dependent s-parameters: S11 is the reflection coefficient of the input cavity mode, S22 is the reflection coefficient of the output cavity mode, and S21 is the transmission coefficient between input and output of the structure. Both modes of the cavity are tuned to the same frequency of 33.192 GHz. In this case isolation between the input and output modes characterized by S21 curve is approximately 51 dB at the frequency of interest (Fig. 2) which was reached without additional tuning paddles.



90 **Figure 2: Microwave properties of TE103 bimodal resonator simulated by CST Suite: S11 (red) - input port reflection coefficient; S22 (black) - output port reflection coefficient; S21 (blue) - transmission coefficient that indicate output-to-input isolation between input and output ports.**

The resonance frequencies of the empty cavity are higher than the spectrometer frequency range and are shifted by the sample in the quartz tube OD = 2.8 mm, $\epsilon = 3.8$ (Rototec-Spintec, USA) down into the 33 – 34.5 GHz range. Microwave performance of the probehead was tested using a network analyzer (ZVA-40 Rohde&Schwarz) at 294 K on a sample of BDPA:PS powder and on a sample of 0.1 mM OXO TEMPO (Sigma-Aldrich GmbH) in toluene at 80 K. The results of the experimental tests on the OXO TEMPO sample are shown in Fig. 3 with traces representing the reflection coefficient S11 of the input mode (a), the reflection coefficient S22 of the output mode (b), and the transmission coefficient S21 which characterizes the input-to-output isolation (c).



100 **Figure 3: a)** Return loss of the probehead input for switch position 1-3; **b)** Return loss of the cavity output when the network analyzer is connected to the output position as indicated in Fig. 1; **c)** Input-to-output isolation of the probehead without the LNA. On the left: input and output modes are tuned to the same frequency of 34.208 GHz. On the right: output mode was detuned to 34.342 GHz (134 MHz above the input mode).

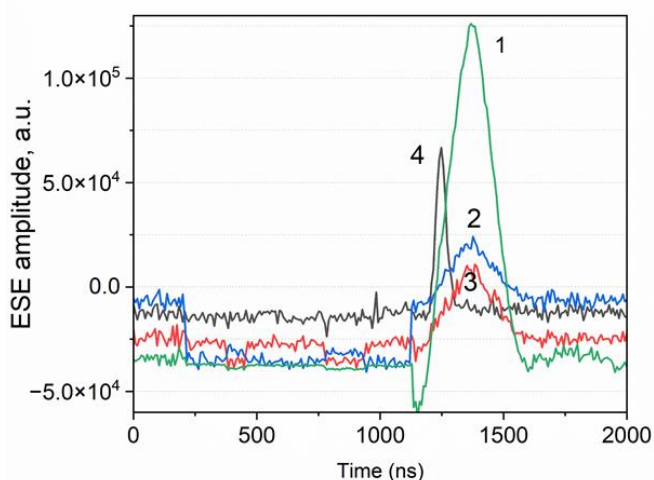
Traces (a) and (b) on the network analyzer screen are return loss traces. Their shift down to ~ 4 dB and ~ 8 dB relative to 0 dB level is due to propagation losses in coaxial cables connecting the probe to the network analyzer and insertion losses in the mw components inside the probe. Trace (c) indicates the minimum isolation at the resonant position. Logically, if the two modes resonate at the same frequency (Fig. 3 on the left), then the isolation will be lower compared to the case of any frequency offset between the two modes (Fig. 3, on the right). In the presented graph a 134 MHz frequency offset between both modes provides higher isolation by 5 dB. This dependence of isolation on frequency offset can be used as a tool for indirectly monitoring the output mode and adjusting it to the frequency of the input mode by means of Xepr on the Bruker ELEXYS E580.



The measured decoupling between the input and output of the resonator is approximately: $(52 \text{ dB} - (4 \text{ dB} + 8 \text{ dB})/2) = 46 \text{ dB}$. This experimental value is few dBs worse than the simulated one due to the imperfections of the inner surfaces of the fabricated resonator structure and due to the presence of a sample tube which may slightly shift from the axis in the experiments.

115

The assembled probehead was tested using electron spin echo (ESE) experiments on a Bruker ELEXYS E580 EPR spectrometer equipped with a 150 W TWT amplifier (Applied Systems Engineering Inc., USA). For testing at room temperature we use BDPA:PS powder with a total of 10^{15} spins in a 0.5 mm ID fused quartz capillary (VitroCom, USA). The sample capillary was placed in the probehead with a 2.8 mm OD sample tube and measured in both reflection and transmission 120 modes when both modes were set to the same frequency. The same sample in the same capillary was also measured with a Bruker EN 5170 D2 probehead. The echo signals of both probeheads (bimodal and Bruker EN 5170 D2), normalized to the same noise level are presented in Fig. 4.



125 **Figure 4: Hahn echo with BDPA:PS in a 0.5 mm ID quartz capillary measured at 294 K in:** 1 – bimodal probehead in transmission mode with LNA (Patt=18 dB; $\pi/2$ -pulses = 80 ns; π -pulses = 160 ns); 2 - bimodal probehead without LNA in reflection mode; 3 - EN 5170 D2 probehead (Patt= 24 dB; $\pi/2$ -pulses = 80 ns; π -pulses = 160 ns); 4 - EN 5170 D2 probehead (Patt= 0 dB; $\pi/2$ -pulses = 6 ns; π -pulses = 12 ns). All traces were recorded with single shot per point, and with 400 ns delay between the pulses.

In the case of the bimodal probehead the mw attenuation was set to 18 dB in order to avoid overload and damage of the LNA that resulted in optimal $\pi/2$ -pulses = 80 ns; π -pulses = 160 ns pulses. A similar pulse sequence was used with the EN 5170 D2 130 probehead, setting mw attenuation to 24 dB. This test showed a 4-fold improvement in the signal-to-noise ratio (SNR) for the bimodal probehead equipped with the LNA. For comparison, full mw power (0 dB attenuation) was also applied to the EN 5170 D2 probehead with optimal $\pi/2$ -pulses = 6 ns; π -pulses = 12 ns pulses. In this case the SNR improvement using the bimodal probe is still 2 times achieved by measuring the peak amplitudes of the echo signals.

We also accomplished another Hahn echo experiment using a 0.1 mM TEMPO in toluene sample in a 2.8 mm OD and a 1.6 135 mm OD sample tubes for the bimodal and Bruker EN 5170 D2 probeheads respectively. This experiment was performed at 80 K. The experimental results of this test are shown in Fig. 5.

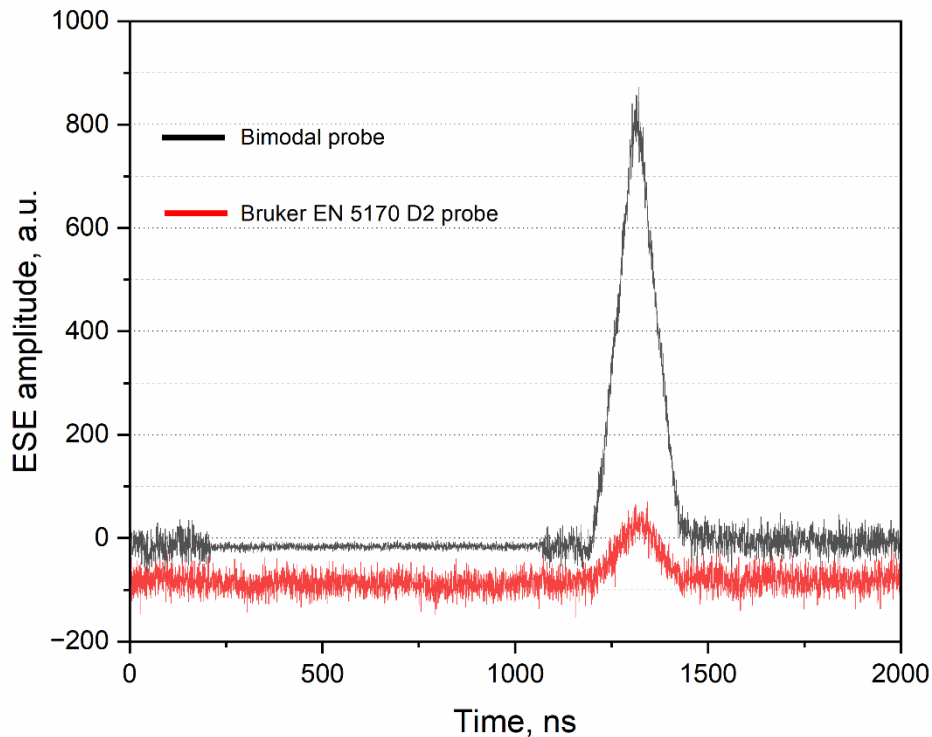


Figure 5: Spin echo with 0.1 mM OXO TEMPO in toluene measured at 80 K by a typical Hahn echo experiment in: blue – a 2.8 mm OD sample tube inside the bimodal probehead (Patt=15 dB; $\pi/2$ -pulses = 50 ns; π -pulses = 100 ns); red – a 1.6 mm OD sample tube inside the EN 5170 D2 probehead (Patt= 22 dB; $\pi/2$ -pulses = 50 ns; π -pulses = 100 ns). All traces were recorded with single shot per point, and with 400 ns delay between the pulses. Video gain is 6 dB.

140

145

In this case signal-to-noise enhancement is reaching factor of 7 but only with a lower mw power and longer pulse lengths. The difference of the results of this test and the previous one is mainly due to larger number of spins in the 2.8 mm OD sample tube used in the bimodal probehead with respect to the 1.6 mm OD sample tube used in the Bruker probehead. It should be noted that the reliability of this comparison depends on the specific performance of the commercial EN 5170 D2 probe. Our EN 5170 D2 probehead is not a new one and may have a slightly lowered mw power conversion factor compared to other (new) commercial probes.

4 Discussion

The aim of this study is a proof-of-principle demonstration of the improvements obtained by using a bimodal resonator combined with a LNA in the detection channel directly after the resonator. There is still the prerequisite to use reduced mw pulse power for the spin excitation due to the limited isolation of 46 dB between the input and output of the mw resonator. This means that at the moment it is not possible to use the full 150 W power of the travelling wave tube amplifier. However, despite the restrictions caused by the modest input-to-output isolation of our newly developed probehead, we were able to



demonstrate a significant SNR enhancement compared to the standard reflection mode operation of the probe, as well as with
155 a commercial Q-band probehead. The developed probehead may be interesting for use in time-resolved EPR methods (Biskup, 2019) that do not require such high mw power. Such methods include transient EPR (Niklas and Poluektov, 2017; Tait et al., 2015) and non-adiabatic rapid scan EPR (NARS) (Kittell et al., 2011; Stoner et al., 2004; Rokeakh and Artyomov, 2023). In addition, for pulse EPR applications with broadband mw pulses the bimodal resonator might offer a significant advantage in avoiding standing waves compared to resonators in the reflection mode (Trenkler et al., 2025).
160 The isolation level can be further improved by introducing tune paddles into the resonator (Mailer et al., 1980), which we plan to do in the future to extend the probe to high mw power. Another improvement will be a cryogenic LNA which is placed into the cryostat to reduce the noise temperature at the input of the LNA from 160 K to supposed 10-50 K (Kalandra et al., 2023) as well as to further reduce the noise figure of the LNA itself. However, the presence of strong magnetic fields can impair the operation of the LNA due to the Hall effect (Harrysson Rodrigues et al., 2019) which should be eliminated by proper shielding
165 from the magnetic field or careful orientation of the LNA. In addition, the problem associated with repeated cooling and warming cycles of the probe can lead to a shorter LNAs lifetime.

5 Conclusions

This work showed that a bimodal cavity in combination with a LNA connected to the mw resonator in transmission mode led to an improvement in SNR in pulse EPR experiments performed at Q-band frequencies. For simplicity the LNA is placed
170 outside the cryostat at room temperature which provides a noise figure of 1.9 dB at 34 GHz. As a result, we achieved an experimental SNR enhancement factor of 2 to 4 regardless of the sample temperature and composition of the sample. Another feature of the proposed probehead is its compatibility with commercial Bruker ELEXYS EPR spectrometers without any modification of the mw bridge.

Data availability

175 The Supplement contains the following files: bimodal cavity simulation TE103_induction.cst that was used to optimize geometry of the structure



Author contribution

180 VD and TP designed the experiments and BE carried them out. VD and AF developed the model and performed the simulations. VD prepared the manuscript with contributions from all co-authors.

Competing interests

At least one of the (co-)authors is a member of the editorial board of Magnetic Resonance.

Acknowledgements

185 We thank the BMRZ for financial support of the EPR infrastructure and the DFG for funding of this project No 471089264. AF thanks financial support from the Institute of Applied Physics RAS under project No FFUF-2024-0027. VD, BE, TP would like to thank Thorsten Maly for the BDPA:PS sample prepared during his stay in the lab.

References

190 Barendswaard, W., Disselhorst, J. A. M., and Schmidt, J.: A bimodal cavity for reducing the dead-time in electron spin-echo spectroscopy, *J. Magn. Reson.*, 58, 477-483, [https://doi.org/10.1016/0022-2364\(84\)90152-5](https://doi.org/10.1016/0022-2364(84)90152-5), 1984.

Bienfait, A., Pla, J., Kubo, Y., Stern, M., Zhou, X., Lo, C. C., Weis, C. D., Schenkel, T., Thewalt, M. L. W., Vion, D., Esteve, D., Julsgaard, B., Moelmer, K., Morton, J. J. L., and Bertet, P., Reaching the quantum limit of sensitivity in electron spin resonance, *Nature Nanotech.*, 11, 253–257, <https://doi.org/10.1038/nnano.2015.282>, 2016.

195 Biskup, T.: Structure–Function Relationship of Organic Semiconductors: Detailed Insights From Time-Resolved EPR Spectroscopy, *Front. Chem.* 7, 10, <https://doi.org/10.3389/fchem.2019.00010>, 2019.

200 Budil, D. E. and Earle, K. A.: Sample Resonators for Quasioptical EPR, in: Very High Frequency (VHF) ESR/EPR. Biological Magnetic Resonance, edited by: Grinberg, O. Y. and Berliner, L. J., Springer, Boston, MA, https://doi.org/10.1007/978-1-4757-4379-1_11, 2004.

205 Forrer, J., Garcí'a-Rubio, I., Schuhmam, R., Tschaggelar, R., and Harmer, J.: Cryogenic Q-band (35 GHz) probehead featuring large excitation microwave fields for pulse and continuous wave electron paramagnetic resonance spectroscopy: Performance and applications, *J. Magn. Reson.*, 190, 280–291, <https://doi.org/10.1016/j.jmr.2007.11.009>, 2008.



Harrysson Rodrigues, I., Niepce, D., Pourkabirian, A., Moschetti, G., Schleeh, J., Bauch, T., and Grahn, J.: On the angular dependence of InP high electron mobility transistors for cryogenic low noise amplifiers in a magnetic field, *AIP Advances*, 9, 085004, <http://doi.org/10.1063/1.5107493>, 2019.

210

Hyde, J.S. and Froncisz, W.: Loop gap resonators, in: *Advanced EPR: Applications in biology and biochemistry*. A. J. Hoff (Ed.). Elsevier, Amsterdam, 277–305, ISBN 0-444-88050-X, 1989.

Hyde, J.S. and Mett, R.R.: EPR uniform field signal enhancement by dielectric tubes in cavities, *Appl. Magn. Reson.*, 48, 215 1185–1204, <https://doi.org/10.1007/s00723-017-0935-4>, 2017.

Hyde, J.S., Chien, J.C.W., and Freed, J.H.: Electron–electron double resonance of free radicals in solution, *J. Chem. Phys.*, 48, 4211–4226, <https://doi.org/10.1063/1.1669760>, 1968.

220

Huisjen, M. and Hyde, J.S.: A pulsed EPR spectrometer, *Rev. Sci. Instrum.*, 45, 669–675, <https://doi.org/10.1063/1.1686710>, 1974.

Jbara, M., Zgadzai, O., Harneit, W., and Blank, A.: Cryogenic W-band Electron Spin Resonance Probehead 225 with an Integral Cryogenic Low Noise Amplifier, *Appl. Magn. Reson.*, 56, 265–284, <https://doi.org/10.1007/s00723-024-01732-1>, 2025.

Kalendra, V., Turcak, J., Banys, J., Morton, J.L., and Šimenas, M.: X- and Q-band EPR with cryogenic amplifiers independent of sample temperature, *Journal of Magnetic Resonance* 346, 107356, <https://doi.org/10.1016/j.jmr.2022.107356>, 2023.

230

Kittell, A. W., Camenisch, T. G., Ratke, J. J., Sidabras, J. W., and Hyde, J. S.: Detection of undistorted continuous wave (CW) electron paramagnetic resonance (EPR) spectra with non-adiabatic sweep (NARS) of the magnetic field, *J. Magn. Reson.*, 211, 228–233, <https://doi.org/10.1016/j.jmr.2011.06.004>, 2011.

235 Mailer, C., Thomann, H., Robinson, B.H., and Dalton, L.R.: Crossed TM_{110} bimodal cavity for measurement of dispersion electron paramagnetic resonance and saturation transfer electron paramagnetic resonance signals for biological materials, *Rev. Sci. Instrum.*, 51, 1714–1721, <https://doi.org/10.1063/1.1136162>, 1980.

Milikisiyants, S., Nevezorov, A.A., and Smirnov, A.I.: Photonic band-gap resonators for high-field/high frequency EPR of 240 microliter-volume liquid aqueous samples. *J. Magn. Reson.* 296, 152–164, <https://doi.org/10.1016/j.jmr.2018.09.006>, 2018.



Neugebauer, P. and Barra, A.-M.: New Cavity Design for Broad-Band Quasi-Optical HF-EPR Spectroscopy, *Appl. Magn. Reson.* 37, 833–843, <https://doi.org/10.1007/s00723-009-0092-5>, 2010.

245 Niklas, J., and Poluektov, O. G.: Charge transfer processes in OPV materials as revealed by EPR spectroscopy. *Adv. Energy Mater.* 7:1602226, <https://doi.org/10.1002/aenm.201602226>, 2017.

Piasecki, W., Froncisz, W., and Hyde, J. S.: Bimodal loop-gap resonator, *Rev. Sci. Instrum.* 67, 1896–1904, <https://doi.org/10.1063/1.1147001>, 1996.

250 Pfenninger, S., Froncisz, W., and Hyde, J. S.: Noise analysis of epr spectrometers with cryogenic microwave preamplifiers, *J. Magn. Reson., Ser. A*, 113, 32–39, <https://doi.org/10.1006/jmra.1995.1052>, 1995.

255 Prisner, T. and Dinse, K. P.: ESR with stochastic excitation, *J. Magn. Reson.*, 84, 296-308, [https://doi.org/10.1016/0022-2364\(89\)90373-9](https://doi.org/10.1016/0022-2364(89)90373-9), 1989.

Raitsimring, A., Astashkin, A., Enemark, J. H., Blank, A., Twig, Y., Song, Y., and Meade, T. J.: Dielectric resonator for K-band pulsed EPR measurements at cryogenic temperatures: probehead construction and applications, *Appl. Magn. Reson.*, 42, 441-452, <https://doi.org/10.1007/s00723-012-0313-1>, 2012.

260 Reijerse, E., Lendzian, F., Isaacson, R., and Lubitz, W.: A tunable general purpose Q-band resonator for CW and pulse EPR/ENDOR experiments with large sample access and optical excitation, *J. Magn. Reson.* 214, 237-243, <https://doi.org/10.1016/j.jmr.2011.11.011> 2012.

265 Rinard, G. A. and Eaton, G.R.: Loop-Gap Resonators, in: *Biomedical EPR, Part B: Methodology, Instrumentation, and Dynamics. Biological Magnetic Resonance*, edited by: Eaton, S. R., Eaton, G. R., Berliner, L. J., 24/B, 19-52, Springer, Boston, MA, https://doi.org/10.1007/0-306-48533-8_2, 2005.

270 Rinard, G. A., Quine, R. W., Ghim, B. T., Eaton, S. S., and Eaton, G. R.: Easily tunable crossed-loop (bimodal) EPR resonator, *J. Magn. Reson. A*, 122, 50-57, <https://doi.org/10.1006/JMRA.1996.0173>, 1996.

Rinard, G. A., Quine, R. W., Song, R., Eaton, G. R., and Eaton, S. S.: Absolute EPR spin echo and noise intensities, *J. Magn. Reson.*, 140, 69–83, <https://doi.org/10.1006/jmre.1999.1823>, 1999.



275 Rokeakh, A. I. and Artyomov, M. Y.: Low-Frequency NARS (LF NARS) by the use of a superheterodyne EPR spectrometer, J. Magn. Reson., 349, 107402, <https://doi.org/10.1016/j.jmr.2023.107402>, 2023.

Šimėnas, M., O'Sullivan, J., Zollitsch, C.W., Kennedy, O., Seif-Eddine, M., Ritsch, I., Hülsmann, M., Qi, M., Godt, A., Roessler, M. M., Jeschke, G., and Morton, J. L.: A sensitivity leap for X-band EPR using a probehead with a cryogenic preamplifier, J. Magn. Reson. 322, 106876, <https://doi.org/10.1016/j.jmr.2020.106876>, 2021.

280 Simovic, B., Studerus, P., Gustavsson, S., Leturcq, R., Ensslin, K., Schumann, R., Forrer, J., and Schweiger, A.: Design of Q-Band loop-gap resonators at frequencies 34–36 GHz for single electron spin spectroscopy in semiconductor nanostructures, Rev. Sci. Instrum. 77 (6), <https://doi.org/10.1063/1.2206776>, 2006.

285 Smith, G., Cruickshank, P., Bolton, D. R., and Robertson, D. A.: High-field pulse EPR instrumentation, Electron Paramagnetic Resonance, 21, 216–233, <https://doi.org/10.1039/b807958g>, 2008.

290 Stoner, J. W., Szymanski, D., Eaton, S. S., Quine, R. W., Rinard, G. A., and Eaton, G. R.: Direct-detected rapid-scan EPR at 250 MHz, J. Magn. Reson., 170, 127–135, <https://doi.org/10.1016/j.jmr.2004.06.008>, 2004.

295 Tait, C. E., Neuhaus, P., Peeks, M. D., Anderson, H. L., and Timmel, C.: Transient EPR Reveals Triplet State Delocalization in a Series of Cyclic and Linear π -Conjugated Porphyrin Oligomers, J. Am. Chem. Soc., 137, 8284–8293, <https://doi.org/10.1021/jacs.5b04511>, 2015.

300 Tesi, L., Bloos, D., Hrtoň, M., Beneš, A., Hentschel, M., Kern, M., Leavesley, A., Hillenbrand, R., Krápek, V., Šikola, T., and van Slageren, J.: Plasmonic Metasurface Resonators to Enhance Terahertz Magnetic Fields for High-Frequency Electron Paramagnetic Resonance, Small Methods, 5(9):e2100376, <https://doi.org/10.1002/smtd.202100376>, 2021.

305 Tipikin, D. S., Earle, K. A., and Freed, J. H.: Variable Coupling Scheme for High-Frequency Electron Spin Resonance Resonators Using Asymmetric Meshes, Appl. Magn. Reson., 37, 819–832, <https://doi.org/10.1007/s00723-009-0088-1>, 2010.

Tkach, I., Sicoli, G., Höbartner, C., and Bennati, M.: A dual-mode microwave resonator for double electron–electron spin resonance spectroscopy at W-band microwave frequencies, J. Magn. Reson., 341–346, <https://doi.org/10.1016/j.jmr.2011.01.012>, 2011.

305 Trenkler, P., Endeward, B., Sigurdsson, S., and Prisner, T.: Optimized shaped pulses for 2D-SIFTER, Magn. Reson. Discuss. [preprint], <https://doi.org/10.5194/mr-2025-11>, in review, 2025.



310 Tschaggelar, R., Breitgoff, F. D., Oberhansli, O., Mian, Qi., Godt A., and Jeschke, G.: High-Bandwidth Q-Band EPR
Resonators, *Appl. Magn. Reson.*, 48, 1273–1300, <https://doi.org/10.1007/s00723-017-0956-z>, 2017.

315 Twig, Y., Dikarov, E., and Blank, A.: Ultra miniature resonators for electron spin resonance: Sensitivity analysis, design and
construction methods, and potential applications, *Mol. Phys.*, 111:18-19, 2674-2682,
<https://doi.org/10.1080/00268976.2012.762463>, 2013.

320 Usevicius, G., Šimenas, M., Geoghegan, B. L., Kennedy, O. W., Pocius, I., Hogan, P., Villanueva Ruiz de Temino, A.,
Verstraete, J.-B., Verbaitytė, P., Chatziathanasiou, A., Antilen Jacob, G., Kamarauskas, M., Treideris, M., Gecys, P.,
Alexander, J., Kalendra, V., Banys, J., Roessler, M. M., and Morton J. L., Versatile High-Sensitivity EPR Using
Superconducting Spiral Microresonators, *Small Methods*, e01451, <https://doi.org/10.1002/smtd.202501451>, 2025.